

See discussions, stats, and author profiles for this publication at: <https://www.researchgate.net/publication/244446234>

Synthesis and Properties of Asymmetric Heteroarm PEO_n-b-PS_mStar Polymers with End Functionalities

ARTICLE *in* MACROMOLECULES · OCTOBER 2004

Impact Factor: 5.8 · DOI: 10.1021/ma0497557

CITATIONS

53

READS

19

8 AUTHORS, INCLUDING:



Maryna Ornatska

Clarkson University

28 PUBLICATIONS 1,381 CITATIONS

SEE PROFILE



Stanislas Petrash

Henkel AG & Co

15 PUBLICATIONS 436 CITATIONS

SEE PROFILE

Synthesis and Properties of Asymmetric Heteroarm PEO_{*n*}-*b*-PS_{*m*} Star Polymers with End Functionalities

S. Peleshanko,[†] J. Jeong,[†] V. V. Shevchenko,[‡] K. L. Genson,[†] Yu. Pikus,[†] M. Ornatska,[†] S. Petrash,[§] and V. V. Tsukruk*,[†]

Department of Materials Science and Engineering, Iowa State University, Ames, Iowa 50011, The Institute of Macromolecular Chemistry, Kiev, 02160, Ukraine, and Corporate Research, National Starch and Chemical Company, Bridgewater, New Jersey 08807

Received February 4, 2004; Revised Manuscript Received July 7, 2004

ABSTRACT: We report on the “core-first” synthesis of asymmetric three- and four-arm poly(ethylene oxide) (PEO)–polystyrene (PS) star polymers with functional terminal groups of a general formula PEO_{*n*}-*b*-PS_{*m*} with *n* = 0, 1, and 2 and *n* + *m* ≤ 4. The synthesis was conducted by anionic polymerization of ethylene oxide and followed by atom transfer radical polymerization (ATRP) of styrene. The properties of asymmetric star-shaped macromolecules with different numbers of arms (*n* = 1; *m* = 2 and 3) and similar lengths of the PEO arm were compared with homoarm star polymers (PEO₄ and PS₄) and corresponding linear polymers. All star polymers obtained here possessed well-defined architecture with a relatively narrow molecular weight distribution as confirmed by NMR, FTIR, and arm-disassembling techniques. Star polymers showed suppression of melting temperature and lower crystallinity PEO phase due to the presence of a junction point. Preliminary studies demonstrated surface activities of these block copolymers with a rich polymorphism of micellar surface structures expected for amphiphilic block copolymers despite the presence of the bulky terminal functionalized groups.

Introduction

In the past years, much attention has been paid to a variety of star shaped polymers with different chemical compositions and well-defined chemical architectures which were synthesized using sophisticated approaches such as anionic polymerization and atom radical transfer polymerization (ATRP).^{1,2} New star block copolymers composed of similar arms (homoarm) and different arms (miktoarm or heteroarm) with different molecular weights and architectures have been synthesized.^{3,4} These polymers are expected to exhibit unique phase behavior and properties due to a combination of heterogeneity of chemical structure and chain branching.^{5,6} They can be used as polymeric surfactants, electrostatic charge reducers, compatibilizers in polymer blending, phase transfer catalysts, and solid polymer electrolytes. Amphiphilic star–block copolymers, which combine hydrophilic and hydrophobic arms, have been a subject of special attention in surface-related applications. Among them, star copolymers containing hydrophilic poly(ethylene oxide) (PEO) and hydrophobic polystyrene (PS) arms stand apart because of the nonionic and highly crystalline nature of the hydrophilic PEO blocks. The amphiphilic nature of these copolymers with incompatible arms gives rise to special properties not only in selective solvents, but also at surfaces and interfaces.⁷

The formation of surface micelles or well-defined surface aggregation at air–water and air–solid interfaces and in solution has been observed for a number of linear PEO–PS diblock copolymers.^{7,8} In contrast, very few papers have been published to date on the interfacial properties of PEO_{*n*}-*b*-PS_{*m*} and (PEO-*b*-PS)_{*n*} star polymers.⁹ Such heteroarm star polymers have

been synthesized by anionic polymerization where the number of arms varied from 2 to 19. As an example, a star polymer with a large number of arms, PEO₁₀–PS₁₀, with the molecular weight of the arms equal to *M*_{PEO} = 25000 and *M*_{PS} = 2300 was synthesized and characterized and its lyotropic liquid crystalline structures were investigated.¹⁰ Another amphiphilic heteroarm PEO–PS star polymer having a low molecular weight of the PEO block (*M*_n < 2500) and symmetrical architecture was reported.^{11,12} The synthesis of other related types of PEO–PS block copolymers, such as (PS)_{2*n*}(PEO)_{*n*}, (PS)_{2*n*},¹³ gemini-like PEO₂-*b*-PS,¹⁴ and Janus-type,¹⁵ have also been discussed. While previous attempts at synthesizing heteroarm star polymers with various architectures have been successful and significant progress has been achieved in the understanding of the bulk microstructure and properties, only limited input on the role of chemical architecture on interfacial properties can be found in the literature.

To date major attention has been paid to star block copolymers with chemical compositions close to symmetrical, which favors the formation of lamellar phases with asymmetrical composition but has been tested only on a few occasions. On the other hand, all star block copolymers synthesized to date possess “dead” terminal groups (e.g., methyl groups) which are not capable of further modification and chemical reactions such as, e.g., those involving grafting of these star polymers to solid substrates and at interfaces. Even in situation when the PS arms possess bromine terminal groups which can be used for further reactions, the PEO arms are completely blocked. This design, thus, prevents any further developments by placing star block copolymers at asymmetrical interfaces and allowing dissimilar arms to be chemically grafted on *both sides of the interfaces*. This kind of interfacial design can be of interest for various, stress-prone applications, and star polymers can be explored as potential adhesives, reinforcing

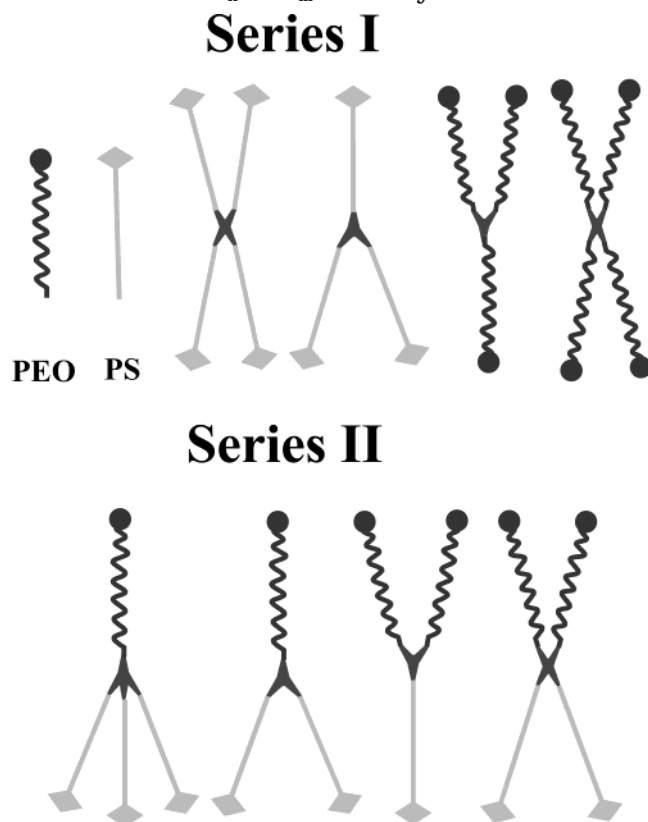
* To whom correspondence should be addressed. E-mail: vladimir@iastate.edu.

[†] Iowa State University.

[‡] The Institute of Macromolecular Chemistry.

[§] National Starch and Chemical Co.

Scheme 1. General Schematics of Star Polymers Synthesized in This Work: Series I, Homoarm Linear and Star Polymers; Series II, Three- and Four-Arm PEO_n-b-PS_m Star Polymers



additives, and components for multilayered protective coatings.^{16,17} Considering this far-reaching target, in our research we focus on synthesis and comprehensive characterization of a series of heteroarm star block copolymers with *both dissimilar arms functionalized with terminal groups* capable of further modification and reaction.

The goal of this particular study reported is the synthesis of a novel series of asymmetric, heteroarm star polymers of the PEO_n-b-PS_m type with both types of arms possessing different terminal functionalities. These functional terminal groups of the both different types of arms can be selectively transformed later in reactive groups suitable, e.g., for grafting the solid substrates or on an asymmetrical interface. Here, we focus on asymmetric, heteroarm star polymers PEO-b-PS₂ and PEO-b-PS₃ with a single PEO arm of modest molecular weight and a variable number and molecular weight of PS arms (Scheme 1). We also synthesize star polymers, PEO₃, PEO₄, and PS₄, as well as symmetric PEO₂-b-PS₂ star polymer for comparative purposes (Figure 1). In this paper, we describe the synthesis of these star block copolymers and the results of the characterization of their chemical composition and bulk properties and include preliminary data on their surface behavior. The detail discussion of their surface properties, morphologies, and microstructures in relationship with their chemical architecture will be published elsewhere.¹⁸

Experimental Procedures

Chemicals. Tetrahydrofuran (THF) was purified by drying over sodium-benzophenone before distillation. Styrene (St) was stored over calcium hydride and then vacuum distilled

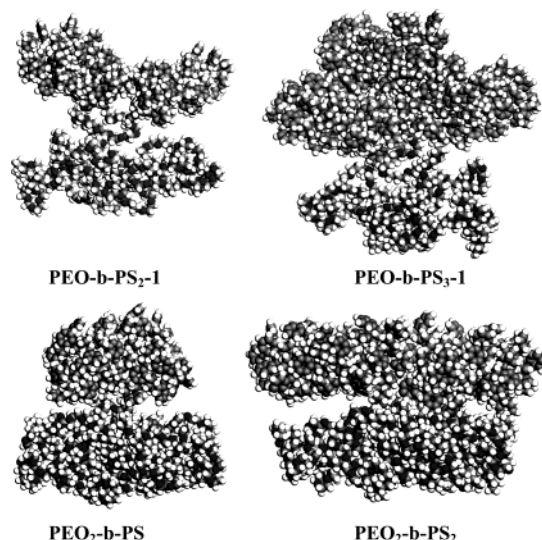
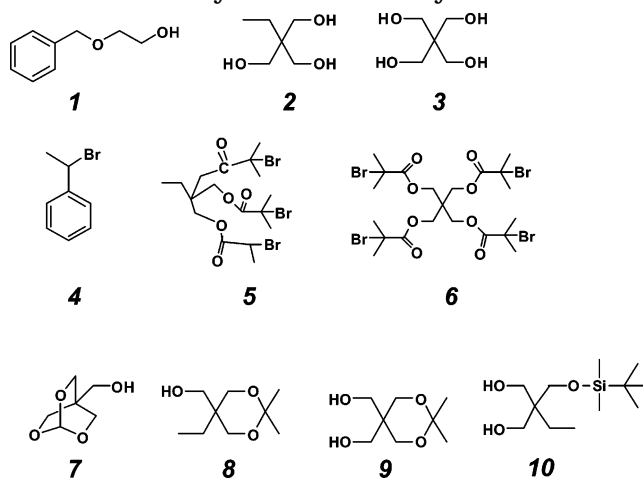


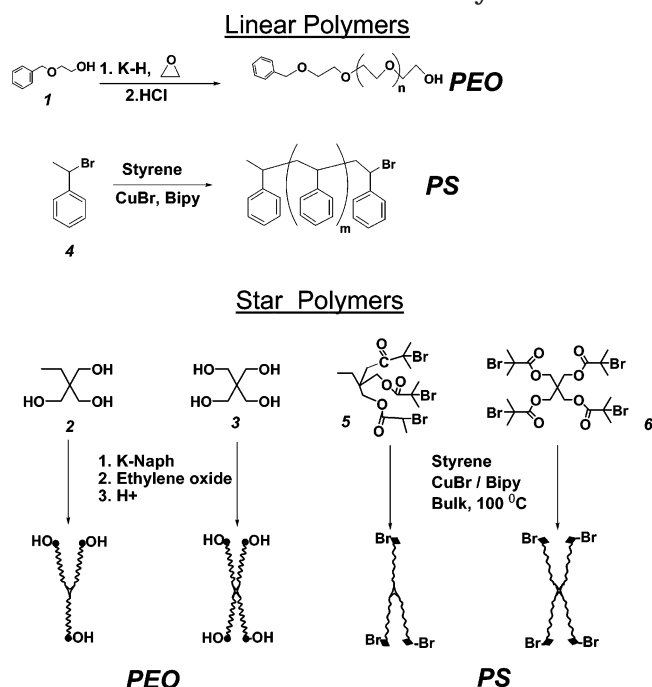
Figure 1. Molecular models of heteroarm star polymers.

Scheme 2. Chemical Structure of Initiators Used for the Synthesis of the Polymers



before use. Ethylene oxide (EO, Aldrich) was purified by stirring over CaH₂ for 3 h before being distilled into a reaction flask. Methylene chloride was distilled over CaH₂. 2-(Benzyloxy)ethanol, **1**, was distilled from calcium hydride. 2,2'-Bipyridine (Bipy, Acros), triethylamine (TEA, Fisher), 2-ethyl-2-hydroxymethyl-1,3-propanediol (trimethylolpropane (TMP), Aldrich), **2**, and pentaerythritol, **3**, were purified according to the literature.¹⁹ Potassium naphthalide (K-Naph) was prepared according described procedure.²⁰ (1-Bromoethyl)benzene, **4**, was distilled under vacuum prior to use. 4-(Dimethylamino)pyridinium-4-toluenesulfonate (DPTS) was prepared according to a known procedure.²¹ Copper(I) bromide (CuBr) was purified according to a reported procedure.²² Methanol (Fisher), hydrochloric acid (aqueous, 12 M, Fisher), 2-bromoisoobutyl bromide (Alfa Aesar), *tert*-butyldiphenylchlorosilane (TBDPS-Cl, Aldrich), *tert*-butyldimethylchlorosilane (TBS-Cl, Aldrich), potassium hydride, potassium, and 4-(dimethylamino)pyridine (DMAP, Acros) were used as received. The initiators, 1,1,1-tris(2-bromo isobutyryloxymethyl)propane (3Br-Pr), **5**,²³ pentaerythritol tetrakis(2-bromo isobutyrate) (4Br-Bu), **6**,^{7,22} 4-(hydroxymethyl)-2,6,7-trioxabicyclo[2.2.2]octane (HTBO), **7**,²⁴ 2,2-dimethyl-5,5-bis(hydroxymethyl)-1,3-dioxane, **8**,²⁵ and 2,2-dimethyl-5,5-bis(hydroxyl methyl)-1,3-dioxane, **9**,²⁶ were synthesized as described in the corresponding references. The 2-(*tert*-butyldimethylsilyloxy)ethanol-2-ethylpropane-1,3-diol, **10**, was synthesized using a well-known procedure that will be briefly presented below. The chemical structures of all initiators are shown in Scheme 2.

Synthesis of 2-(*tert*-butyldimethylsilyloxy)ethanol-2-ethylpropane-1,3-diol, **10 (Scheme 2).** Dry triethylamine

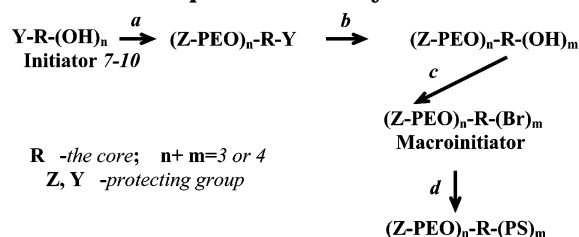
Scheme 3. Synthetic Path Used for the Synthesis of Homoarm Linear and Star Polymers**Table 1. GPC Molecular Characteristics of Linear and Homoarm Star Polymers**

polymer structure		M_n	M_w	PDI
linear PS	1	7200	9300	1.29
	2	8800	10700	1.22
linear PEO	1	6330	6840	1.08
	2	8690	9250	1.06
3-arm star PEO		25120	30220	1.2
4-arm star PEO		50130	63320	1.26
3-arm star PS	1	17440	19840	1.13
	2	49000	52950	1.08
4-arm star PS	3	58500	64220	1.09
	1	20310	22050	1.08
	2	45560	48950	1.07

(13 g, 17.5 mL, 130 mmol) and a catalytic amount of (dimethylamino)pyridine (2.8 g, 98 mmol) were added to a solution of TMP (2) (15.7 g, 117 mmol) in 120 mL of dry THF. TBS-Cl (1 M solution in THF, 40 mL, 40 mmol) was added, and the mixture was stirred for 48 h at room temperature. The reaction solution was diluted with 200 mL of CH₂Cl₂ and washed with 200 mL of saturated NH₄Cl (4×) and 200 mL of water (2×). The organic phase was dried over MgSO₄ and concentrated to yield 26 g of a transparent orange liquid. The crude product was purified by column chromatography on silica gel with ethyl acetate/hexane (3:7) to yield **10** as a transparent colorless liquid (11.6 g, 40% yield). ¹H NMR (CDCl₃, δ): 0.00 (s, 6H, -SiCH₃), 0.74 (q, 3H, -CH₂-CH₃), 0.92 (s, 9H, -CH₃), 1.41 (t, 2H, -CH₂-CH₃), 2.96 (m, 1H, -OH), 3.41 and 3.54 (d, 2H, -CH₂O-), 3.48–3.69 (d, 2H, -CH₂O-).

Synthesis of Linear and Star PEO Polymers. Linear and star PEO polymers were synthesized by deprotonation of hydroxyl groups of the initiator followed by polymerization of ethylene oxide in THF at 45 °C (Scheme 3) according to well-established procedures.^{27,28} ¹H NMR of the linear PEO (δ, ppm, CDCl₃): 7.3–6.3 (m, 5H, aromatic); 3.6 (s, 4H, (CH₂CH₂O)_n PEO block). The molecular characteristics of the linear and homoarm star polymers synthesized at this stage are presented in Table 1.

Synthesis of PEO Blocks of Heteroarm Star Polymer. The PEO_n-b-PS_m star polymers were obtained in four steps using the protected initiators presented in Scheme 2. The general synthetic route is presented in Scheme 4. Step a is anionic polymerization of EO. Step b is removing protecting

Scheme 4. A General Routine for the Synthesis of Heteroarm Star Polymers Used in This Work: Step a, Anionic Polymerization of EO; Step b, Deprotection; Step c, Synthesis of Br-Terminated PEO Precursor; Step d, ATRP of Styrene

groups of the polymer under mild acidic condition in methanol. In step c, the ω-bromo-PEO precursors were obtained after reaction with 2-bromoisobutyl bromide in THF. Step d is atom transfer radical polymerization (ATRP) using styrene as a monomer in the presence of CuBr/bipyridyl system as a catalyst.

Deprotection of the hydroxyl groups of the initiator using potassium naphthalide was followed by the polymerization of ethylene oxide in THF at 45 °C as described in the literature.²⁸ Instead of using an acidic solution, the anionic polymerization was terminated by adding the TBDPS-Cl (1.5 equiv), TEA (2 equiv), and DMAP (0.2 equiv) to the reaction flask. The reaction mixture was stirred for another 24 h at 40 °C. After cooling, the mixture concentrated on rotor evaporator, then precipitated in diethyl ether (three times), dried and store in the refrigerator at +2°. The final yield was 85–90%. ¹H NMR results of synthesized PEO blocks of PEO_n-b-PS_m macroinitiator (δ, ppm, CDCl₃): **PEO-b-PS₃**, 7.3–6.3 (m, 10H, aromatic), 5.5 (s, 1H), 3.6 (s, 4H, (CH₂CH₂O)_n PEO block), 1.05 (s, 9H, C(CH₃)₃); **PEO-b-PS₂**, 7.3–6.3 (m, 10H, aromatic), 3.6 (s, 4H, (CH₂CH₂O)_n PEO block), 1.43 (q, 2H, -CH₂-CH₃), 1.32 ppm (s, 6H), 1.05 (s, 9H, C(CH₃)₃), 0.78 (t, 3H, -CH₂-CH₃); **PEO₂-b-PS₂**, 7.3–6.3 (m, 20H, aromatic), 3.6 (s, 4H, (CH₂CH₂O)_n PEO block), 1.32 ppm (s, 6H), 1.05 (s, 18H, C(CH₃)₃); **PEO₂-b-PS**, 7.3–6.3 (m, 20H, aromatic), 3.6 (s, 4H, (CH₂CH₂O)_n PEO block), 1.43 (q, 2H, -CH₂-CH₃), 1.05 (s, 27H, C(CH₃)₃), 0.78 (t, 3H, -CH₂-CH₃), 0.05 (s, 6H, -Si(CH₃)₃).

Deprotection of the PEO Block. First, 1 g of PEO macroinitiator was dissolved in 3 mL of the 80% acetic acid solution in THF. The reaction mixture was stirred for 2 h at room temperature. The polymers were precipitated twice in ether and dried under a high vacuum for 12 h (yield was 80%). Cleavage of the protecting groups was monitored by the changing intensity of the peak in the ¹H NMR spectra at 5.5 ppm for PEO-b-PS₃ macroinitiator, at 1.32 ppm for PEO-b-PS₂ and PEO₂-b-PS₂, and at 0.05 ppm for PEO₂-PS macroinitiator.

Synthesis of Macroinitiators for Heteroarm Star Polymers. The ω-bromo-PEO precursors were obtained after reacting of the deprotected PEO block of the heteroarm star polymer with 2-bromoisobutyl bromide in THF. The last step was performed using ATRP of styrene as a monomer in the presence of the CuBr/bipyridyl system as a catalyst.

Under typical reaction conditions, the polymer with deprotected OH groups was chemically modified by 2-bromoisobutyl bromide in the presence of TEA. First, 1 g (0.14 mmol) of bromo-functionalized PEO macroinitiator ($M_n = 7300$) was dissolved under an argon atmosphere in a solution of 1 mL of TEA in 50 mL of anhydrous THF. After this, 0.2 mL (54 mmol, 10 equiv) of 2-bromoisobutyl bromide was added dropwise at 0 °C (ice bath) over 15 min with vigorous stirring. The mixture was then stirred overnight at room temperature. The triethylamine hydrobromide was precipitated, and after filtration, the solution was concentrated by evaporation and poured in 10-fold excess of diethyl ether. After filtration, the precipitate was dissolved in a small amount of dry THF, centrifuged to remove residual salt, and precipitated one more time. The final yield was 80%. The degree of functionalization was monitored by the appearance of ¹H NMR signal at 1.9 ppm, which corresponds to the OOC(CH₃)₂Br group.

Synthesis of Linear, Star PS and PS Blocks of Star Polymers. Linear and star PS polymers were synthesized by the reaction of the hydroxyl groups of the polyols with 2-bromoisobutryl bromide in THF, followed by ATRP of the obtained initiator with styrene as a monomer in the presence of CuBr/Bipyridine (Bipy) catalyst at 100 °C (Scheme 2).^{12,29} A Schlenk flask was charged with tris(2-bromoisobutryrate) PEO macroinitiator **3** (0.2 g, 3.33×10^{-5} mol), CuBr (13.2 mg, 1×10^{-4} mol), and Bipy (46.8 mg, 3×10^{-4} mol). Styrene (2.1 mL, 2.2×10^{-2} mol) was added, and the mixture was degassed and heated at 100 °C for 6 h. Dichloromethane was added to the crude product, and the mixture was filtered over a column of neutral alumina. The resulting solution was precipitated twice in a large excess of hexane. The polymer was dried under vacuum at 30 °C. ¹H NMR results for PEO-*b*-PS₃ and PEO₂-*b*-PS star polymers (δ , ppm, CDCl₃): 7.3–6.3 (m, PS block, aromatic), 3.6 (s, 4H, (CH₂CH₂O)_{*n*}, PEO block), 2.5–1.1 (m, 3H, PS block, aliphatic main chain), 1.0 (s, 9H, C(CH₃)₃).

Hydrolysis of the PEO_{*n*}-*b*-PS_{*m*} and PS_{*n*} Copolymers. The character of the branched architectures was verified by the cleavage of ester functions linking the PEO moiety to PS arm and analyzing the molecular weight of cleaved arms. The procedure was conducted in accordance with that described in the literature.³⁰ Typically, the star polymer (50 mg, 7.2×10^{-5} mol of ester) was dissolved in THF (10 mL). Then, KOH (1 mL, 1 M in methanol solution) was added via a syringe. The solution was refluxed overnight. After this, the solution was concentrated by the evaporation of THF and precipitated in pure methanol (yield of 40%).

Characterization. ¹H NMR spectra were recorded with a 300 MHz Bruker spectrometer with a solvent proton signal as the internal standard. The number-average molecular weight (*M_n*) of the PS and PEO chains were calculated from ¹H NMR spectra using the ratio of the aromatic protons (δ = 6.2–7.2) and the oxirane (–OCH₂–) protons of the ethylene oxide unit (δ = 3.6) against *tert*-butyl protons (δ = 1.05), respectively. Gel permeation chromatography (GPC) measurements in THF were performed in HPLC-grade THF at a flow rate of 1 mL/min using a Waters Breeze GPC system equipped with a Waters 1515 pump, Waters 717/plus auto-sampler, and Waters 2414 RI-detector. A set of two columns (PL-Gel Mixed C 5 μ m, Polymer Lab., Inc.) with gradient of pore sizes from 100 to 10⁵ Å was used for these measurements. The column calibration procedure used PS standards (Polymer Lab., Inc.) having a narrow molecular weight distribution. A polymer sample was dissolved in THF with concentration around 0.5–1.5 mg/mL and filtrated through a Teflon 0.2 μ m filter into a sample vial.

The solid substrates used for the deposition of the block copolymers were freshly cleaned, atomically smooth, [100] silicon wafers of high quality used in our previous studies of various monolayers and grafted polymers.^{31,32} Wafer preparation was conducted in a class 100 Cleanroom to avoid air contaminations in accordance with the standard procedure adapted in our laboratory.³³ Polymers adsorbed onto bare silicon surfaces were prepared by submerging a solid substrate in the polymer solution with concentration about 10^{–6}–10^{–7} mol/L for 24 h. After the substrate was washed twice with the solvent used for the preparation of the polymer solution, sample was dried under the stream of nitrogen. Langmuir–Blodgett (LB) monolayer deposition was conducted using an LB trough (R&K 1, Germany). Then 45–60 μ L of dilute polymer solution (concentration about 0.1 mmol/L) in chloroform was deposited onto the Nanopure water surface of the LB trough, and the solvent was left to evaporate for 30 min. After this, the monolayer was compressed to a specific pressure and deposited onto a silicon substrate while simultaneously keeping the surface pressure constant. The surface morphology was observed with atomic force microscopes (AFM) Dimension-3000 and Nanoscope III Multimode microscopes (Digital Instruments, Inc.) in the tapping mode according to the usual procedure adapted in our laboratory.^{34,35}

DSC analyses were performed on an MDSC Q100 instrument and a Perkin-Elmer 7 series thermal analysis system with a heating rate of 20 °C/min. Approximately 5 mg of

polymers was used for these measurements. The X-ray measurements of bulk polymers were performed on a Scintag XDS-2000 X-ray diffractometer. Scans were collected in the 2θ range from 5 to 35°, with a step of 0.05°, and a scan rate of 0.5°/min. The generator parameters were set at 45 kV with the current of 35 mA. Monochromatic Cu K α radiation with a wavelength of 1.54 Å was used for all measurements. All peaks observed in diffraction pattern were fit using a Lorentzian function. The degree of crystallinity was calculated by dividing the area beneath all crystalline peaks by the sum of the area beneath all crystalline and amorphous peaks. The molecular models of all molecules were built with the Materials Studio 3.0 software package by using the combination of molecular dynamics and energy minimization routines.

Result and Discussion

Synthesis of the Polymers. Figure 1 shows molecular models generated for all block copolymers synthesized here. The molecular models visualize spatial distribution of two different blocks in molecules with different chemical compositions including those with predominant content of PS blocks and close content of both blocks.

The ¹H NMR spectra of the heteroarm PEO-*b*-PS₃-2 star polymer collected during end functionality transformations are used here for the illustration of controlled chemical step-by-step synthesis procedure implemented in this study (Figure 2). All characteristic peaks expected for the chemical groups of PEO and PS are clearly marked, according to the literature value.³⁶ The appearance of appropriate peaks for various functional groups at different stages of the synthetic procedure is clearly marked at these plots (Figure 2). The relative content of PEO and PS chains was calculated by the integrating of the aromatic signal for the PS backbone and a signal at 1.05 ppm which is related to the *tert*-butyl protons of the TBDPS-protecting group. The calculated parameters for the chemical composition of the star polymers from NMR data are presented in Table 2. As seen from the data, the molecular weight of PEO arms was kept virtually constant and close to 7000 (the degree of polymerization (DP) of about 180) for all star polymers. In contrast, the molecular weight of the PS block varied widely from as low as 9800 to as high as 24000 (DP from 94 to 240). Resulting total molecular weight of the star polymers ranged from 23000 to 67000 (Table 2). This covers the entire range of molecular weights of the selected reference linear blocks (from 6000 to 34000) and homoarm PS and PEO star–block copolymers (from 17000 to 180 000) (Tables 1 and 2).

FTIR was used for independent confirmation of the chemical composition in the bulk state after precipitation from solution. As an example, the spectrum of PEO-*b*-PS₃-2 heteroarm star copolymer is presented in Figure 3. The peak at 2850 cm^{–1} corresponds to CH₂ and CH stretching vibration of PS backbones.³⁷ The presence of the phenyl groups of PS chains is confirmed by strong peaks at 700 and 3000–3200 cm^{–1}, which correspond to the deformational and stretching vibrations of the aromatic C–H bond. That also is confirmed by two strong peaks at 1450 and 1500 cm^{–1} corresponding to the deformation vibration of C–C bonds of the aromatic ring. A strong peak at 2900 cm^{–1} and a broad peak around 1100 cm^{–1} confirmed the presence of CH₂ and C–O–C ether group of PEO units (Figure 3). The variation of the peak intensities for CH₂ and CH(ar) groups was used for independent qualitative control of the chemical composition for heteroarm star copolymers.

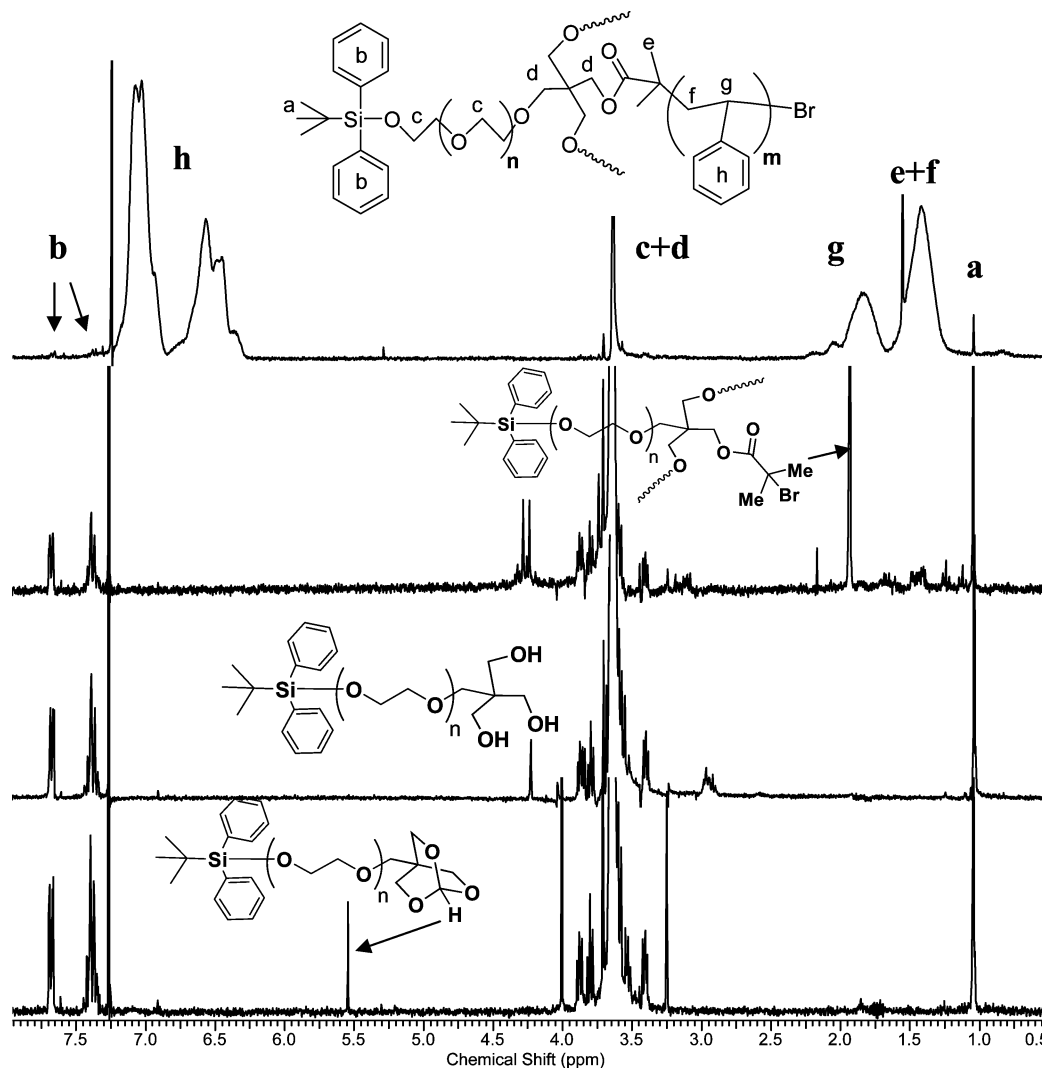


Figure 2. ^1H NMR spectra of end functionality transformations for all major intermediate steps in the course of the synthesis of PEO-*b*-PS₃-2 heteroarm star polymer with the assignment of major peaks.

Table 2. Chemical Composition^a and Molecular Weight of Heteroarm Star Polymers

polymer	GPC data						NMR data			
	PEO arm		PS arm (after cleavage)		total		PEO arm		PS arm	total
	M_n	PDI	M_n	PDI	M_n	PDI	M_n	φ_{PEO}^d	M_n	M_n
PEO- <i>b</i> -PS ₃ -1 ^a	7100	1.09	10200	1.1	23300	1.16	7500	0.18	9800	37000
PEO- <i>b</i> -PS ₃ -2 ^b	7100	1.09	18300	1.13	38200	1.19	7500	0.10	20000	67000
PEO- <i>b</i> -PS ₂ -1 ^a	7200	1.05	7900	1.16	19200	1.29	7100	0.26	8900	25000
PEO- <i>b</i> -PS ₂ -2 ^b	7200	1.05	26900	1.15	47400	1.18	7100	0.11	23900	54800
PEO ₂ - <i>b</i> -PS ^b	5600	1.13	9400	1.17	20000	1.2	6300	0.53	9800	22500
PEO ₂ - <i>b</i> -PS ₂ ^c	6300	1.1	14300	1.23	19200	1.16	6300	0.31	13900	40900

^a Time = 6 h. ^b Time = 12 h. ^c Time = 8 h. ^d φ is the volume fraction of a PEO block. ^e Styrene:–Br group:CuBr:Bipy = 300:1:1:3.

The progress in synthesis of the linear and star homopolymers and the quality of the final molecular weight distribution were also controlled by GPC (Figure 4). As expected, the PEO linear chains possessed very narrow molecular weight distribution (PDI < 1.1) and the PEO star polymers showed only slightly higher PDI around 1.1–1.2 (Table 1). PDI for PS linear and star polymers obtained with ATRP were in the same range varying from 1.1 to 1.3. All heteroarm star polymers showed a relatively low polydispersity (usually below 1.2) (Table 2). Although, the absolute value of the molecular weight cannot be directly determined from GPC because of the specific solution properties caused by nonlinear architecture of the polymer chains,^{6,38} but

the GPC data showed an important general trend consistent with the NMR data with fairly close but underestimated absolute values (Table 2). The difference between GPC and NMR data is usually observed for highly branched polymers and is related to the different conformational of star polymers as compared to linear chains from calibration standards.³⁹

The GPC curves were obtained for all intermediate products to control even subtle changes in the molecular structure at different synthetic stages. For example, a control for the synthesis of the PEO-*b*-PS₃-2 star polymer (Table 2) is shown in Figure 4. As can be clearly seen from the data, the polydispersity remained low and unchanged during the deprotection of the initially

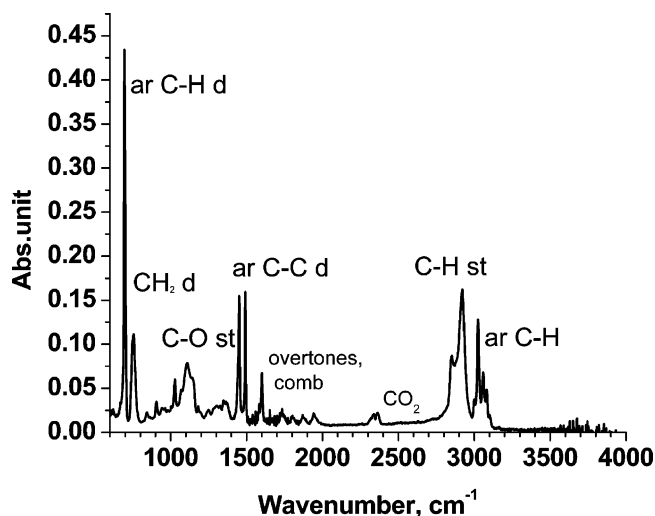


Figure 3. FTIR data for the heteroarm PEO-*b*-PS₃-2 star polymer with the assignment of all major peaks.

synthesized PEO chains and their quenching with 2-bromoisobutyryl bromide in the presence of triethylamine. The GPC plot after the polymerization of styrene showed the formation of PS arms as confirmed by the proportional shift of the peak (Figure 4). The initial peak corresponding to the precursor disappeared completely,

which indicated that all PEO macroinitiator molecules were consumed in the course of the reaction. The presence of a new peak, which appeared after at a much shortened elution time, confirmed the formation of the star polymer.

The final independent and critical confirmation of the actual architecture of the star polymers came from the star disassembling technique widely used for these polymers.¹² The hydrolysis of the star polymers and following GPC analysis of the cleaved arms were conducted as recommended by Gnanou et al. (Figure 4).¹² The results presented in Table 2 for the cleaved PS chains provided crucial confirmation of the actual star architecture. The molecular weight of both PEO chains obtained independently before synthesis of star polymers and PS arms cleaved from the star structure were very close (usually within $\pm 10\%$) to that estimated from NMR data for the original star polymers (Table 2). GPC data also demonstrated a narrow molecular weight distribution of the cleaved arms with PDI below 1.2 for PS chains. Therefore, a combination of several chemical characterization techniques and cleavage technique provided clear evidence of the formation of the star architecture as intended for these polymers.

Thermal Properties. It is well-known that the suppression of the melting temperature is usually observed for the PEO phase in star polymers. This

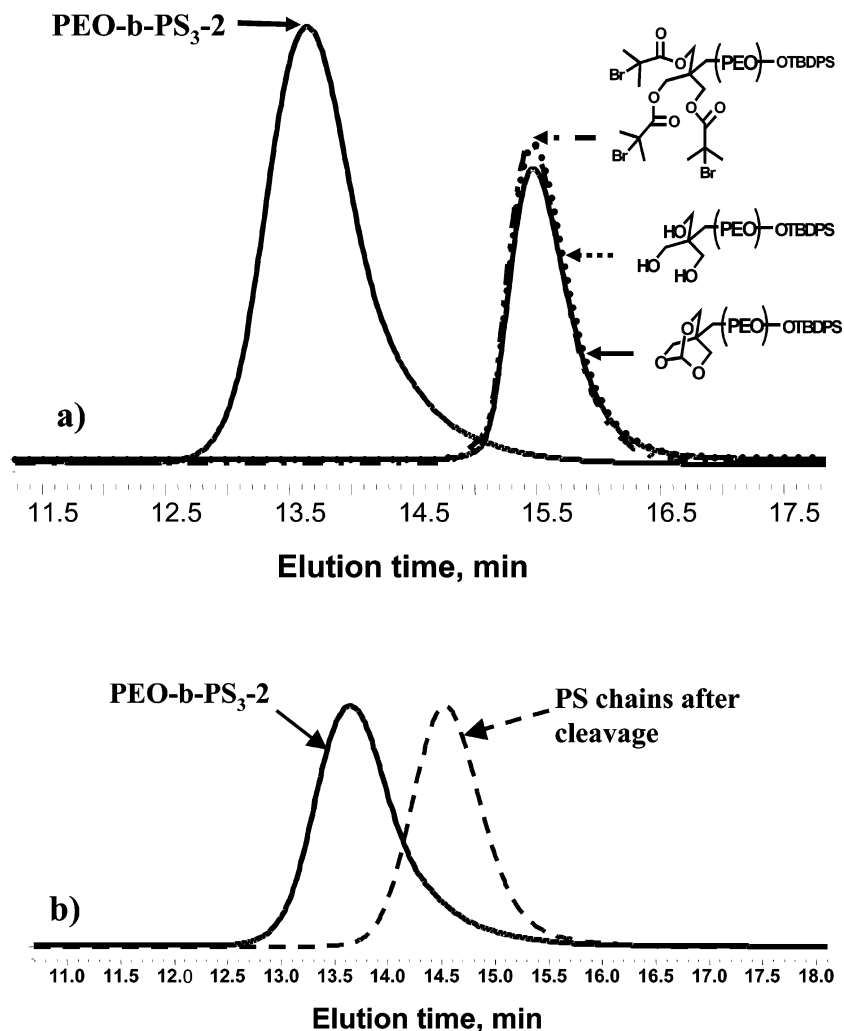


Figure 4. GPC data for of intermediate steps in the course of the synthesis of PEO-*b*-PS₃-2 heteroarm star polymer: (a) (1) PEO-block after polymerization; (2) PEO-block after deprotection; (3) PEO-(Br)₃ macroinitiator; (4) resulting PEO-*b*-PS₃-2 star polymer; (b) resulting heteroarm PEO-*b*-PS₃-2 star polymer (solid line) and PS fragments after cleavage (dash line).

Table 3. Thermal Data of Selected Heteroarm Star Polymers^a

polymer	<i>T</i> _g (PS), °C	<i>T</i> _m (PEO), °C	ΔH , J/g	overall α , %	PEO phase α , %
PEO- <i>b</i> -PS ₃ -2	94	61	4.5	2.4	24
PEO- <i>b</i> -PS ₂ -2	91	62.5	9.1	4.5	40

^a ΔH is the enthalpy of melting of the polymer. The overall α is the degree of crystallinity, calculated from DSC: $\alpha = (\Delta H / \Delta H_f) \times 100\%$, where $\Delta H_f = 188$ J/g^{9a} is the enthalpy of melting of PEO. PEO phase α = overall $\alpha / \varphi_{\text{PEO}}$ and is characteristic of the PEO phase itself.

phenomenon is attributed not only to the lower molecular weight of the PEO arms but also to the presence of the core, which makes a more defective crystal structure where the central core is excluded from the PEO crystal lattice.^{40,41} In fact, our data confirmed a similar trend for the heteroarm star polymers synthesized in the course of this work. DSC experiments performed on several selected samples in the temperature range from -80 to $+150$ °C showed very similar results for different architectures (see typical data in Table 3). The peak melting temperature, *T*_m, of PEO chains was shifted to lower temperatures as compared to the *T*_m = 66 °C observed for a linear polymer.⁴² Overall, this shift was fairly similar for all star polymers studied here and varied from 3 to 6 °C. The melting peak of the PEO-enriched phase in the star polymer exhibited a modest broadening, which may be attributed to the higher polydispersity of the star polymers.

We calculated the apparent overall degree of crystallinity in star polymers from the DSC data and obtained very low values ranging from 2.4% to 4.5% (Table 3). This is partially due to the low fraction of PEO blocks usually present in these materials. However, these values were well below the expected values estimated from the volume fraction of the PEO arms. In fact, the estimated degree of crystallinity of the PEO phase itself calculated by taking into account the PEO content in the material was relatively modest and not exceeding 40% (Table 3). This is well below usual values obtained for linear PEO polymers. As is known, linear PEO shows excellent crystallization properties with the degree of the crystallinity reaching 90–95%.^{43,44}

The DSC results also confirmed that a well-defined microphase separation between PEO and PS arms takes place in the heteroarm star polymer, as expected for a bicomponent system in a strong segregation limit.⁴⁵ In addition to the exothermic peak corresponding to the melting of the PEO phase discussed above, the glass transition of the PS chains was detected at elevated temperatures. Again, the glass transition temperature was slightly lower (10–20 °C) than that seen for linear, high molecular weight PS.⁴² The lowering of the glass transition temperature of the PS chains observed here is in agreement with the known trends for linear polymers with lower molecular weight. This phenomenon can be enhanced by the presence of the branch points as was suggested for star-shaped PS polymers with different cores and the number of PS arms.^{46–48}

Crystalline Structure. The crystalline structure of the PEO phase was modestly affected by the molecular architecture in a similar way as the thermal properties discussed above. The X-ray data for the linear PEO polymers synthesized here were similar to those observed earlier for the high molecular weight PEO with only a slight reduction in intensity being observed for the major peaks. This indicates a slightly reduced

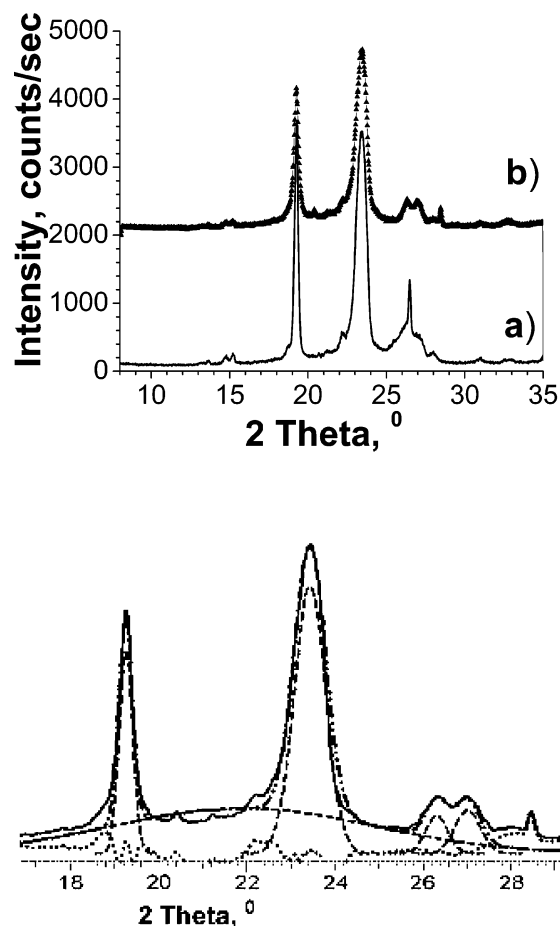


Figure 5. Top: X-ray diffraction data for linear PEO polymer *M*_n = 8690 (a) and 4-arm PEO star polymer (b). Bottom: peak fitting of the XRD data of the four-arm PEO star polymer: XRD data of the star polymer (solid); crystalline and amorphous peak fitting (dash); calculated fitting (dash dot dot); difference between calculated and initial XRD data (dot).

Table 4. Parameters of the Unit Cell and the Degree of Crystallinity of Selected Polymers

polymer	<i>a</i> , Å	<i>b</i> , Å	<i>c</i> , Å	<i>d</i> , Å	α , %
PEO, lit. data ⁴²	8.05	13.04	19.5		92
linear PEO, <i>M</i> _n = 8690	8.03	13.06	19.4		67
4-arm PEO star polymer	7.98	13.1	17.9		55
PS, literature data ⁴²	0	0	0	4.54	0
4-arm PS star polymer	0	0	0	4.79	0
PEO- <i>b</i> -PS ₃ -1	0	0	0	4.55	<5
PEO- <i>b</i> -PS ₃ -2	0	0	0	4.43	<5
PEO- <i>b</i> -PS ₂ -2	0	0	0	4.48	<5

crystalline order in the shorter PEO chains. In fact, the comparison of literature data and the calculated values of unit cell parameters in the monoclinic crystal structure and the degree of crystallinity, α , showed virtually unchanged unit cell parameters but a lower degree of crystallinity of the linear, low molecular weight PEO (Table 4). This change can be associated with a slightly increased polydispersity seen for PEO chains synthesized here and the presence of the bulky terminal groups (see Scheme 3).

A relatively high degree of crystallinity is usually observed for PEO homoarm star polymers as well.⁴¹ Indeed, an X-ray plot for the 4-arm PEO homoarm star polymer synthesized here displayed a number of sharp peaks (Figure 5).⁴⁹ Two major peaks with the highest intensities at $2\theta = 19$ and 23° correspond to the reflections from [120] and [032] + [112] crystallographic

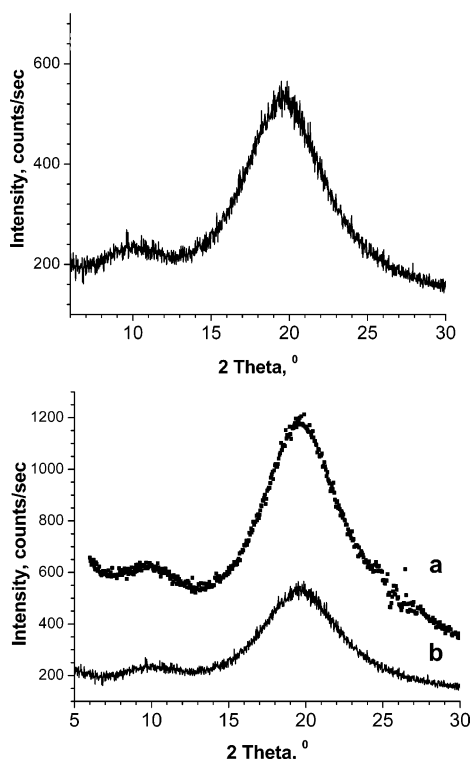


Figure 6. X-ray diffraction data for linear PS chain (top) and heteroarm star polymers PEO-*b*-PS₃-1 (bottom, a) and PEO-*b*-PS₃-2 (bottom, b).

planes of the monoclinic unit cell, respectively.⁵⁰ In this unit cell, the PEO macromolecules assume a helical conformation consisting of seven monomer units per the identity period of 19.48 Å (Figure 4).⁵¹

The peak fitting was used for the separation of crystalline and amorphous contributions and the calculation of the degree of crystallinity as demonstrated in Figure 5. The homoarm star polymer with the same molecular weight of the individual PEO chains displayed the reduced degree of crystallinity to 55% as compared to the linear PEO chains synthesized here (Table 4). This known effect is due to the presence of the junction point in the star polymers and the restricted mobility of the PEO arms as was suggested earlier.⁵² It is worth noting that the parameters of the PEO crystal lattice strongly depend on sample thermal history and crystallization conditions; however, this was not the focus of the current study.^{53–55}

For linear PEO-*b*-PS diblock copolymers it has been shown that the confinement of crystalline lamellae between amorphous phases frequently results decreased crystallinity.⁵⁶ Similar behavior was in fact observed for the PEO-PS star polymers synthesized here. X-ray diffraction data for the PS star polymer showed two diffuse maxima around 10 and 20° that corresponded to the amorphous structure of linear PS materials with short-range ordering of the backbones and side groups (Figure 6).⁵⁷ The similar *d* spacing and diffuse character of the diffraction maxima indicated unchanged amorphous structure of the PS chains in star polymers.

Very similar diffraction data with two diffuse maxima were obtained for two different PEO-*b*-PS₂ heteroarm star polymers (Figure 6). No signs of sharp peaks indicating the presence of the PEO phase were detected for either polymer (we estimated the low limit of the detectable degree of crystallinity under our experimental conditions to be close to 5%). Considering the high

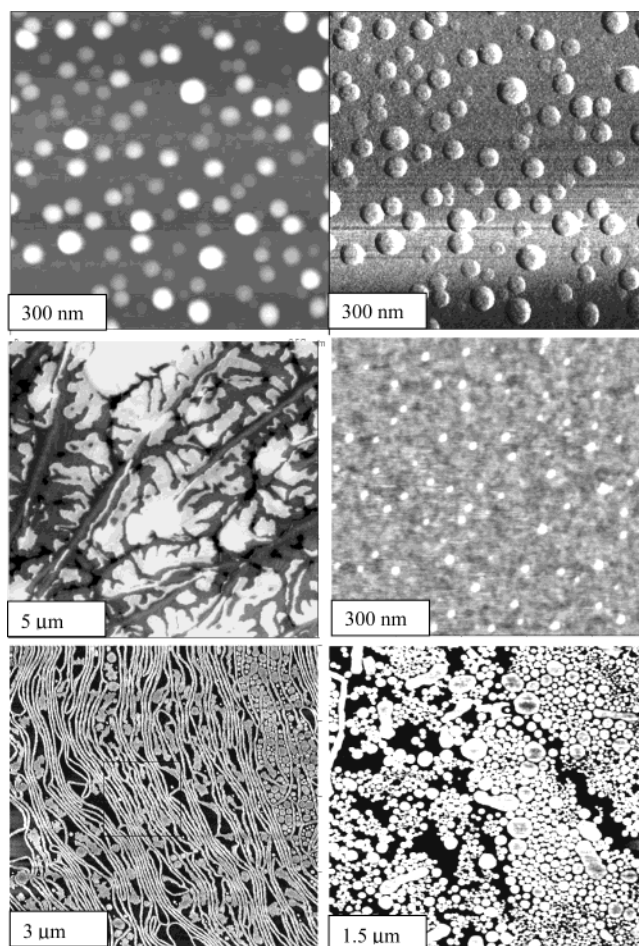


Figure 7. Spherical micellar structures of adsorbed PEO-*b*-PS₃-2 from toluene. Top: topographical (left) and phase (right) images. Scan size is $1 \times 1 \mu\text{m}^2$; height scale is 40 nm, phase scale is 10°. Middle: adsorbed PEO-*b*-PS₂-2 from chloroform (right, scan size $1 \times 1 \mu\text{m}^2$, height scale 6 nm) and dendritic crystalline structures of PEO₄ cast from THF (left, scan size $15 \times 15 \mu\text{m}^2$, height scale 50 nm). Bottom: lamellar and circular micellar structures Langmuir monolayer of PEO-*b*-PS₃-2 formed at different surface pressure (left, 5 mN/m near meniscus, scan size $10 \times 10 \mu\text{m}^2$, height scale 10 nm; right, 0 mN/m near center, scan size $5 \times 5 \mu\text{m}^2$, height scale 5 nm).

intensity and the large width of the diffuse maxima caused by predominant PS phase (the volume fraction of 74–90%), we estimated that the content of crystalline PEO crystal phase did not exceed 5%. Thus, we can conclude that the crystallinity of the PEO phase itself in these heteroarm star polymers should not exceed 20–50% according to X-ray data. This is consistent with the DSC evaluation discussed above (Table 3). Apparently, the presence of several PS arms attached to the same core resulted in even more pronounced suppression of the PEO crystallization than that observed for the homoarm star polymers. On the other hand, the presence of the bulky functional groups attached to the very ends of the PEO chains (Figure 2) could disturb crystallization process and slightly lower the degree of crystallinity of relatively short PEO chains.

Surface Behavior: Preliminary Results. Preliminary studies of the surface behavior of the PEO-*b*-PS_{*m*} star polymers synthesized here revealed a strong trend to form micellar structures while cast from a solution onto the silicon wafer and the air–water interface (Langmuir monolayers) (Figure 7). We observed the formation of dendritic crystalline structures for the PEO

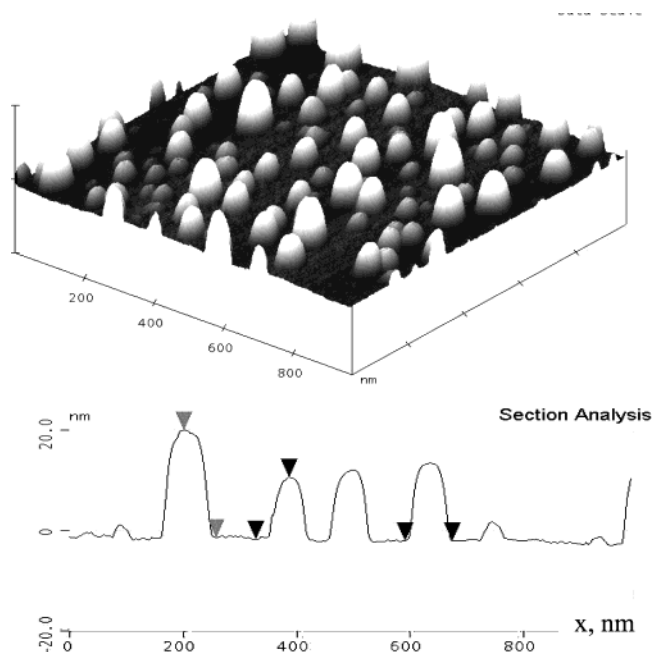


Figure 8. 3D AFM topographical image of micellar structures of adsorbed PEO-PS₃-2 and corresponding cross-section. Scan size is $1 \times 1 \mu\text{m}^2$; height scale is 40 nm.

star polymers and stable spherical nanoscale micelles on a hydrophilic surface even when a nonselective solvent is used (Figure 7). The height of the micellar structures usually did not exceed 10 nm and lateral dimensions were below 80 nm indicating the formation of micellar structures formed from a limited number of molecules (Figure 7). Moreover, the amphiphilic heteroarm star polymers synthesized here formed stable Langmuir monolayers with a variety of intralayer micellar structures of lamellar and circular types, which was controlled by the initial solution concentration and the surface pressure at the air–water interface (Figure 8). A strong trend to micellar structure formation has been already reported for PEO-*b*-PS star copolymers and other amphiphilic linear block copolymers.^{58,59} However, we observed some peculiar behavior on surface morphologies and microstructures of heteroarm star copolymers as will be discussed in detail in a separate publication.¹⁸

Conclusions

A combination of the anionic polymerization of ethylene oxide and ATRP of styrene was exploited to synthesize novel asymmetrical, amphiphilic PEO-*b*-PS star block copolymers of various architectures with terminal functional groups. Both arms of these star copolymers unlike the known examples are capable of further chemical reaction if placed at asymmetrical interfaces. Most star copolymers synthesized here possessed a single PEO arm of the same molecular weight and a variable number of PS arms with different molecular weights. The synthetic pathway followed to prepare such copolymers enabled us to control both the functionality and the amphiphilic balance with high accuracy. The well-defined character of these branched architectures was verified upon the cleavage of the ester functions linking the PEO moiety to the PS arms. The PS arms obtained as a result of hydrolysis and disassembling of star polymers had low polydispersity and their molecular weights were in a good agreement with

the values calculated by NMR for the corresponding heteroarm star polymers.

For heteroarm star polymers synthesized here, we observed depressed melting temperature and reduced crystallinity of the PEO phase, lower glass transition temperature of the PS blocks, and micellar structure formation at surfaces, all expected for the amphiphilic block copolymers with several arms attached to a single junction point. The presence of the bulky functional groups as terminal groups of PEO blocks can be held as responsible for further reduction of the degree of crystallinity of these molecules. Furthermore, selective modifications of two different end groups of the dissimilar arms in the heteroarm star polymers can cause a broad variation of the chemical and physical properties without any changes of the polymer chain or molecular weight as will be pursued in further studies. This is an interesting aspect for the selective absorption and grafting of heteroarm star polymers placed at the asymmetric interfaces.

Acknowledgment. Funding from Imperial Chemical Industries, SRF 2112 Contract, and the National Science Foundation, Grant DMR-0074241, is gratefully acknowledged. The authors thank R. Gunawidjaja, J. Holzmüller, and B. Rybak for technical assistance.

References and Notes

- (1) (a) *Applications of anionic polymerization research*; Quirk, R. P., Ed.; ACS Symposium Series 696; American Chemical Society: Washington, DC, 1998. (b) Hsieh, H. L.; Quirk, R. P. *Anionic polymerization: principles and practical applications*; Marcel Dekker: New York, 1996.
- (2) (a) *Controlled Radical Polymerization*; Matyjaszewski, K., Ed.; ACS Symposium Series 685. American Chemical Society: Washington, DC, 1998. (b) *Controlled-living radical polymerization: Progress in ATRP, NMP, and RAFT*; Matyjaszewski, K., Ed.; ACS Symposium Series 768. American Chemical Society: Washington, DC, 2000. (c) *Handbook of Radical polymerization*; Matyjaszewski, K., Davis, T. P., Eds.; John Wiley & Sons: New York, 2002.
- (3) (a) Hadjichristidis, N. *J. Polym. Sci., Part A: Polym. Chem.* **1999**, *37*, 857. (b) Hedrick, J. L.; Trollsås, M.; Hawker, C. J.; Atthoff, B.; Heise, A.; Miller, R. D. *Macromolecules* **1998**, *31*, 8691. (c) Glauser, T.; Stancik, C. M.; Moeller, M.; Voytek, S.; Gast, A. P.; Hedrick, J. L. *Macromolecules* **2002**, *35*, 5774. (d) Bosman, A. W.; Vestberg, R.; Heumann, A.; Fréchet, J. M. J.; Hawker, G. J. *J. Am. Chem. Soc.* **2003**, *125*, 3831.
- (4) (a) Ishizu, K.; Uchida, S. *Prog. Polym. Sci.* **1999**, *24*, 1439. (b) Heise, A.; Trollsås, M.; Magbitang, T.; Hedrick, J. L.; Frank, C. W.; Miller, R. D. *Macromolecules* **2001**, *34*, 2798.
- (5) (a) Yung, R. J. *Trends Polym. Sci.* **1997**, *5*, 4. (b) Yoo, M.; Heise, A.; Hedrick, J. L.; Miller, R. D.; Frank, C. W. *Macromolecules* **2003**, *36*, 268. (c) Stancik, C. M.; Pople, J. A.; Trollsås, M.; Lindner, P.; Hedrick, J. L.; Gast, A. P. *Macromolecules* **2003**, *36*, 5765.
- (6) (a) *Star and Hyperbranched Polymer*; Mishra, M. K.; Kobayashi, S., Eds.; Marcel Dekker: New York, 1999. (b) Kanaoka, S.; Nakata, S.; Yamaoka, H. *Macromolecules* **2002**, *35*, 4564. (c) Voulgaris, D.; Tsitsilianis, C.; Grayer, V.; Esselink, F. J.; Hadziioannou, G. *Polymer* **1999**, *40*, 5879. (d) Sotiriou, K.; Nannou, A.; Velis, G.; Pispas, S. *Macromolecules* **2002**, *35*, 4106.
- (7) Xie, H.-Q.; Xie, D. *Prog. Polym. Sci.* **1999**, *24*, 275.
- (8) (a) Yu, K.; Eisenberg, A. *Macromolecules* **1996**, *29*, 6359. (b) Yu, K.; Eisenberg, A. *Macromolecules* **1998**, *31*, 3509.
- (9) (a) Tsitsilianis, C.; Papanagopoulos, D.; Lutz, P. *Polymer* **1995**, *36*, 3745. (b) Francis, R.; Skolnik, A. M.; Carino, S. R.; Logan, J. L.; Underhill, R. S.; Angot, S.; Taton, D.; Gnanou, Y.; Duran, R. S. *Macromolecules* **2002**, *35*, 6483.
- (10) Tsitsilianis, C.; Alexandridis, P.; Lindman, B. *Macromolecules* **2001**, *34*, 5979.
- (11) Taton, D.; Cloutet, E.; Gnanou, Y. *Macromol. Chem. Phys.* **1998**, *199*, 2501.
- (12) Angot, S.; Taton, D.; Gnanou, Y. *Macromolecules* **2000**, *33*, 5418.

- (13) Francis, R.; Taton, D.; Logan, J. L.; Masse, P.; Gnanou, Y.; Duran, R. S. *Macromolecules* **2003**, *36*, 8253.
- (14) Gibanel, S.; Forcada, J.; Heroguez, V.; Schappacher, M.; Gnanou, Y. *Macromolecules* **2001**, *34*, 4451.
- (15) Heroguez, V.; Gnanou, Y.; Fontanille, M. *Macromolecules* **1997**, *30*, 4791.
- (16) (a) Tsukruk, V. V. *Prog. Polym. Sci.* **1997**, *22*, 247. (b) Tsukruk, V. V. *Adv. Mater.* **2001**, *13*, 95. (c) Luzinov, I.; Minko, S.; Tsukruk, V. V. *Prog. Polym. Sci.* **2004**, *29*, 635. (d) Kovalev, A.; Shulha, H.; Lemieux, M.; Myshkin, N.; Tsukruk, V. V. *J. Mater. Res.* **2004**, *19*, 716. (e) Jiang, C.; Markutsya, S.; Tsukruk, V. V. *Adv. Mater.* **2004**, *16*, 157.
- (17) (a) Sidorenko, A.; Ahn, Hyo-Sok; Kim, Doo-In; Yang, H.; Tsukruk, V. V. *Wear* **2002**, *252*, 946. (b) Tsukruk, V. V.; Sidorenko, A.; Yang, H. *Polymer* **2002**, *43*, 1695. (c) Tsukruk, V. V.; Ahn, H.-S.; Sidorenko, A.; Kim, D. *Appl. Phys. Lett.* **2002**, *80*, 4825. (d) Bliznyuk, V. N.; Everson, M. P.; Tsukruk, V. V. *J. Tribology* **1998**, *120*, 489.
- (18) Peleshanko, S.; Jeong, J.; Gunawidjaja, R.; Tsukruk, V. V. *Macromolecules* **2004**, *37*, 6511.
- (19) Armarego, W. L. F.; Perrin, D. D. *Purification of laboratory chemicals*; Butterworth-Heinemann: Oxford, England, 1996.
- (20) Choi, K. C.; Bae, Y. H.; Kim, S. W. *Macromolecules* **1998**, *31*, 8766.
- (21) Würsch, A.; Möller, M.; Glauser, T.; Lim, L. S.; Voytek, S. B.; Hedrick, J. L. *Macromolecules* **2001**, *34*, 6601.
- (22) Matyjaszewski, K.; Miller, P. J.; Pyun, J.; Kickelbick, G.; Diamanti, S. *Macromolecules* **1999**, *32*, 6526.
- (23) Narita, M.; Nomurat, R.; Tomita, I.; Endo, T. *Polym. Bull. (Berlin)* **2000**, *45*, 231.
- (24) Padias, A. B.; Hall, H. K., Jr.; Tomalia, D. A.; McConnell, J. R. *J. Org. Chem.* **1987**, *52*, 5305.
- (25) Six, J.-L.; Gnanou, Y. *Macromol. Symp.* **1995**, *95*, 137.
- (26) Vanderberg, E. J.; Tian, D. *Macromolecules* **1999**, *32*, 3613.
- (27) Reed, N. N.; Janda, K. D. *J. Org. Chem.* **2000**, *65*, 5843.
- (28) (a) Comanita, B.; Noren, B.; Roovers, J. *Macromolecules* **1999**, *32*, 1069. (b) Yilmaz, F.; Cianga, I.; Ito, K.; Senyo, T.; Yagci, Y. *Macromol. Rapid Commun.* **2003**, *24*, 316.
- (29) Matyjaszewski, K.; Xia, J. *Chem. Rev.* **2001**, *101*, 2921.
- (30) Angot, S.; Murthy, K. S.; Taton, D.; Gnanou, Y. *Macromolecules* **1998**, *31*, 7218.
- (31) (a) Zhai, X.; Peleshanko, S.; Klimenko, N. S.; Genson, K. L.; Vortman, M. Ya.; Shevchenko, V. V.; Vaknin, D.; Tsukruk, V. V. *Macromolecules* **2003**, *36*, 3101. (b) Larson, K.; Vaknin, D.; Villavicencio, O.; McGrath, D. V.; Tsukruk, V. V. *J. Phys. Chem.* **2002**, *106*, 7246. (c) Larson, K.; Vaknin, D.; Villavicencio, O.; McGrath, D. V.; Tsukruk, V. V. *J. Phys. Chem.* **2002**, *106*, 11277. (d) Lee, M.; Kim, J.-W.; Peleshanko, S.; Larson, K.; Yoo, Y.; Vaknin, D.; Markutsya, S.; Tsukruk, V. V. *J. Am. Chem. Soc.* **2002**, *124*, 9121. (e) Peleshanko, S.; Sidorenko, A.; Larson, K.; Villavicencio, O.; Ornatska, M.; McGrath, D. V.; Tsukruk, V. V. *Thin Solid Films* **2002**, *406*, 233. (f) Sidorenko, A.; Houphouet-Boigny, C.; Villavicencio, O.; McGrath, D. V.; Tsukruk, V. V. *Thin Solid Films* **2002**, *410*, 147.
- (32) (a) Ko, H.; Peleshanko, S.; Tsukruk, V. V. *J. Phys. Chem.* **2004**, *108*, 4385. (b) Tsukruk, V. V.; Ko, H.; Peleshanko, S. *Phys. Rev. Lett.* **2004**, *92*. (c) Ornatska, M.; Jones, S. E.; Naik, R. R.; Stone, M.; Tsukruk, V. V. *J. Am. Chem. Soc.* **2003**, *125*, 12722. (d) Julthongpipit, D.; Lin, Y.-H.; Teng, J.; Zubarev, E. R.; Tsukruk, V. V. *J. Am. Chem. Soc.* **2003**, *125*, 15912. (e) Tsukruk, V. V.; Shulha, H.; Zhai, H. *Appl. Phys. Lett.* **2003**, *82*, 907.
- (33) Tsukruk, V. V.; Bliznyuk, V. N. *Langmuir*, **1998**, *14*, 446.
- (34) Tsukruk, V. V. *Rubber Chem. Technol.* **1997**, *70*, 430.
- (35) Tsukruk, V. V.; Reneker, D. H. *Polymer*, **1995**, *36*, 1791.
- (36) Pouchert, C. J.; Behnke, J. *The Aldrich Library of ¹³C and ¹H FT-NMR Spectra*; Aldrich Chemical: Milwaukee, WI, 1992.
- (37) Workman, J. *Handbook of Organic Compounds*; Academic Press: San Diego, CA, 2001.
- (38) (a) de Gennes, P. G. *Scaling Concept in Polymer Physics*; Cornell University Press: Ithaca, NY, 1979. (b) Pitsikalis, M.; Pispas, S.; Mays, J. W.; Hadjichristidis, N. *Adv. Polym. Sci.* **1998**, *135*, 1. (c) Hadjichristidis, N.; Pispas, S.; Pitsikalis, M.; Iatrou, H.; Vlahos, C. *Adv. Polym. Sci.* **1999**, *142*, 71.
- (39) (a) Brochard-Wyart, F.; de Gennes, P. G. *C. R. Acad. Sci. Paris* **1996**, *323*, 473. (b) Gay, C.; Raphaël, E. *Adv. Colloid Interface Sci.* **2001**, *94*, 229.
- (40) Chen, E. *Polymer* **1999**, *40*, 4543.
- (41) Chen, E. *Macromolecules* **1999**, *32*, 4784.
- (42) Brandrup, J.; Immergut, E. H.; Grulke, E. A. *Polymer Handbook*; John Wiley & Sons: New York, 1999.
- (43) Cheng, S. Z. D.; Barley, J. S.; Zhang, A.; Habenschuss, A.; Zchack, P. R. *Macromolecules* **1992**, *25*, 1453.
- (44) Cheng, S. Z. D.; Wunderlich, B. *J. Polym. Sci., Polym. Phys. Ed.* **1986**, *24*, 595.
- (45) (a) Zhu, L.; Chen, Y.; Zhang, A.; Calhoun, B. H.; Chun, M.; Quirk, R. P.; Cheng, C. Z. D.; Hsiao, B. S.; Yeh, F.; Hashimoto, T. *Phys. Rev. B* **1999**, *60*, 10022. (b) Zhu, L.; Cheng, S. Z. D.; Calhoun, B. H.; Ge, Q.; Quirk, R. P.; Thomas, E. L.; Hsiao, B. S.; Yeh, F.; Lotz, B. *Polymer* **2001**, *42*, 5829. (c) Reining, B.; Keul, H.; Höcker, H. *Polymer* **2002**, *43*, 7145.
- (46) Roovers, J. E. L.; Toporowsky, P. M. *J. Appl. Polym. Sci.* **1974**, *18*, 1685.
- (47) Knauss, D. M.; Al-Muallem, H. A.; Huang, T.; Wu, D. T. *Macromolecules* **2000**, *33*, 3557.
- (48) Knauss, D. M.; Huang, T. *Macromolecules* **2003**, *36*, 6036.
- (49) Takahashi, Y.; Tadokoro, H. *Macromolecules* **1973**, *6*, 672.
- (50) Tadokoro, H.; Chatani, Y.; Yoshihara, T.; Tahara, S.; Murahashi, S. *Macromol. Chem.* **1964**, *109*.
- (51) (a) Wunderlich, B. *Macromolecular physics*; Academic Press: New York, 1973; Vol. 1. (b) Takahashi, Y.; Tadokoro, H. *Macromolecules* **1973**, *6*, 672.
- (52) Mihaylova, M. D.; Kreteyev, V. P.; Kreteyeva, M. N.; Amzil, A.; Berlinova, I. V. *Eur. Polym. J.* **2001**, *37*, 233.
- (53) Price, F. P.; Kilb, R. W. *J. Polym. Sci.* **1962**, *57*, 395.
- (54) Tadokoro, H. *J. Polym. Sci., Part C* **1966**, *15*, 1.
- (55) Bortel, E.; Hodorovicz, S.; Lamot, R. *Macromol. Chem.* **1979**, *180*, 2491.
- (56) Wang, C.; Zhang, G.; Zhang, Z.; Chen, X.; Tang, X.; Tan, H. *J. Appl. Polym. Sci.* **2003**, *89*, 3432.
- (57) (a) Wignall, G. D.; Hendricks, R. W.; Koehler, W. C.; Lin, J. S.; Wai, M. P.; Thomas, E. L.; Stein, R. S. *Polymer* **1981**, *22*, 886. (b) O'Reilly, J. M.; Stein, R. S.; Hadzioannou, G.; Wignall, G. D. *Polymer* **1983**, *24*, 1255. (c) King, J. S.; Boyer, W.; Wignall, G. D.; Ullman, R. *Macromolecules* **1985**, *18*, 709.
- (58) (a) Hickl, P.; Ballauff, M.; Jada, A. *Macromolecules* **1996**, *29*, 4006. (b) Cogan, K. A.; Gast, A. P. *Macromolecules* **1990**, *23*, 745. (c) Goncalves da Silva, A. M.; Simoes Gamboa, A. L.; Martinho, J. M. G. *Langmuir* **1998**, *14*, 5327. (d) Cox, J. K.; Yu, K.; Constantine, B.; Eisenberg, A.; Lennox, B. R. *Langmuir* **1999**, *15*, 7714. (e) Faure, M. C.; Bassereau, P.; Lee, L. T.; Menelle, A.; Lheveder, C. *Macromolecules* **1999**, *32*, 8538.
- (59) (a) An, S. W.; Su, T. J.; Thomas, R. K.; Baines, F. L.; Billingham, N. C.; Armes, S. P.; Penfold, J. *J. Phys. Chem. B* **1998**, *102*, 387. (b) Baker, S. M.; Leach, K. A.; Devereaux, C. E.; Gragson, D. E. *Macromolecules* **2000**, *33*, 5432. (c) Rivillon, S.; Muñoz, M. G.; Monroy, F.; Ortega, F.; Rubio, R. *Macromolecules* **2003**, *36*, 4068.

MA0497557